Solitary Pulmonary Nodule on Helical Dynamic CT Scans: Analysis of the Enhancement Patterns Using a Computer-Aided Diagnosis (CAD) System

Eun Jung Choi, MD[1]
Gong Yong Jin, MD[1]
Young Min Han, MD[1]
Young Sun Lee, MD[1]
Keun Sang Kweon, MD[2]

Departments of Radiology[1] and Province[2],
Chonbuk National University Hospital and
Medical School, Research Institute for
Medical Science, Chonbuk 561-712,
Korea

Address reprint requests to:
Gong Yong Jin, MD, Department of
Diagnostic Radiology, Chonbuk National
University Medical School, Research
Institute of Clinical Medicine, 634-18
Keumam-dong, Jeonju, Chonbuk 561-
712, Korea.
Tel. (8263) 250-2307
Fax. (8263) 272-0481
e-mail: gyjin@chonbuk.ac.kr

Abbreviations:
CAD = computer-aided diagnosis
DLP = Dose Length Product
NE = net enhancement
NPV = negative predictive value
PE = peak enhancement
PPV = positive predictive value
ROI = region of interest
SPNs = solitary pulmonary nodules
TAC = time attenuation curve

Objective: We wanted to investigate the usefulness of a computer-aided diagnosis (CAD) system in assisting radiologists to diagnosis malignant solitary pulmonary nodules (SPNs), as compared with diagnosing SPNs with using direct personal drawing.

Materials and Methods: Forty patients with SPNs were analyzed. After the pre-contrast scan was performed, an additional ten series of post-contrast images were obtained at 20-second intervals. Two investigators measured the attenuation values of the SPNs: a radiologist who drew the regions of interest (ROIs), and a technician who used a CAD system. The Bland and Altman plots were used to compare the net enhancement between a CAD system and direct personal drawing. The diagnostic characteristics of the malignant SPNs were calculated by considering the CAD and direct personal drawing and with using Fisher's exact test.

Results: On the Bland and Altman plot, the net enhancement difference between the CAD system and direct personal drawing was not significant (within $\pm$ 2 standard deriation). The sensitivity, specificity, positive predictive value (PPV), negative predictive value (NPV) and accuracy of diagnosing malignant SPNs using CAD was 92%, 85%, 75%, 96% and 88%, respectively. The sensitivity, specificity, PPV, NPV and accuracy of diagnosing malignant SPNs using direct drawing was 92%, 89%, 79%, 92% and 88%, respectively.

Conclusion: The CAD system was a useful tool for diagnosing malignant SPNs.

S olitary pulmonary nodules (SPNs) are a major concern not only for radiologists, but also for clinicians because 30–80% of resected SPNs are found to be malignant (1–6). The role of the radiologist for evaluating SPNs is to accurately distinguish between benign and malignant lesions. In general, CT has high specificity and acceptable sensitivity and accuracy, and it might be a reasonable modality for characterizing nodules (1–11). Malignant nodules tend to enhance substantially more than benign nodules even though some overlap, such as for active granulomas or benign vascular tumors, has been found (2, 4, 5, 7, 12–14). More recently, several authors have attempted to assess the washout characteristics of SPNs on contrast-enhanced CT, which is also known as helical dynamic CT (HDCT) (10, 15–17). Jeong et al. (15) evaluated solitary pulmonary nodules by analyzing the combined wash-in and washout characteristics of dynamic contrast-enhanced multi-detector row CT, and they reported 92% accuracy for distinguishing between benign and malignant nodules.

However, a diagnosis of SPNs using HDCT is a difficult task for human readers

because this method requires considerable time to calculate the SPN enhancement and to draw the region of interest (ROI) for all the enhancing nodules on the CT images. Therefore, a computer-aided diagnosis (CAD) system has great potential to resolve this problem. Some studies reported that a CAD system that uses volumetric and contrast-enhanced data has the potential to assist radiologists in differentiating solitary pulmonary nodules and managing these patients (18–23).

A CAD system can usually evaluate the quantitative features of the nodule's size, shape and attenuation. In addition, these systems can calculate the enhancement properties of SPNs on HDCT. This study was designed to determine the usefulness of a CAD system for assisting radiologists in differentiating between benign and malignant SPN by analyzing the enhancement patterns of SPNs on dynamic CT scans. For this study, after comparing a CAD system with direct personal measurement of SPNs on dynamic CT, we evaluated the accuracy of diagnosing malignant SPNs with using a CAD system.

MATERIALS AND METHODS

Patients and CT Scanning

This study was performed retrospectively with the approval of the ethics committee at our institution. Written informed consent was obtained from all patients. From November 2005 to May 2006, a total of 75 patients (50 men and 25 women, mean age, 60 years; age range, 25–79 years), who had a SPN seen on their chest radiography and there was no satellite nodule on the targeted thin-section CT scans (0.75 mm collimation, 0.5-second gantry rotation time, 120 kVp, 50 mA) that were done on the SPN, underwent dynamic chest CT with a sixteen-detector row CT scanner (Somatom Sensation 16, Siemens, Erlangen, Germany). The nodules were excluded if they contained benign calcifications (diffuse, laminated, popcorn-like or central), ground glass opacity, the SPN was less than 5 mm and the nodules were juxtapleura/juxtavascular nodules as seen on the thin-section CT. Patients with heart disease or respiratory difficulties during the inspiration period of CT were also excluded. Of the 75 patients, 35 patients were excluded: 13 patients were lost to follow-up and 22 patients were followed up without a biopsy. Overall, a total of 40 patients with SPNs (29 men and 11 women, mean age, 56.3 years; age range, 25–79 years) that had proven pathology were analyzed. The average long and short axis diameters of the malignant SPNs were 20.6 ± 6.4 mm (12–30 mm) and 17.0 ± 6.1 mm (9–30 mm), respectively. The average long and short axis diameters of the benign SPNs were 16.2 ± 7.2 mm (7–30 mm) and

12.0 ± 4.9 mm (6–23 mm), respectively. Thirty-one patients underwent a percutaneous needle biopsy and nine patients underwent surgery that included a wedge resection.

Before intravenously injecting the contrast medium, a series of images was obtained throughout the entire nodule along the z-axis with 0.75 mm collimation (120 kVp, 170 mA, 0.5 second gantry rotation time). Thereafter, an additional ten series (20s, 40s, 60s, 80s, 120s, 140s, 160s, 180s, 240s and 300s) of images were obtained at 20-second intervals over a 5-minute period after injecting the contrast medium (3 mL/sec, a total of 120 mL of Ultravist® 300; Scherring, Berlin, Germany) with a power injector (MCT Plus; Medrad, Pittsburgh, PA). Immediately after the dynamic imaging, low-dose (Effective mA: 50–60 mAs, 120 kVp, 0.75 mm collimation) helical CT scans were obtained from the lung apices to the level of the middle pole of both kidneys for tumor staging. The image data was reconstructed with a thickness of 2.0 mm and using a standard algorithm. All the thin-sections and dynamic CT data were interfaced directly to our picture archiving and communication system (PACS, m-view™; Marotech, Korea), which displayed all the image data on monitors (four monitors, $1,536 \times 2,048$ image matrices, 8-bit viewable gray scale and 60-foot-lambert luminescence). Both the mediastinal (window width: 400 HU, window level: 20 HU) and lung (window width: 1,500 HU, window level: –700 HU) window images were viewed on the monitor. The technical adequacy of dynamic CT fulfilled the following criteria that were reported by previous studies (14): no extravasated contrast medium at the injection site, appropriate enhancement of the cardiovascular structures during the examination, no reaction to the contrast medium that interfered with image acquisition and satisfactory patient respiratory registration without artifacts on the images.

Radiation Exposure

The total organ doses of the thin-section, dynamic and low-dose CT studies were calculated. An effective patient dose from a chest CT examination is calculated by multiplying the Dose Length Product (DLP) by the conversion factor (25). The DLP is the CT dose index (CTDIvol) multiplied by the scanned length. To establish an effective dose for an examination from the DLP, the conversion factors that are used are age, the scanned region, and specific CT geometry. Generally, the conversion factor for adult patients undergoing chest CT examinations is 0.017 mSv per mGy cm. The average calculated mean effective dose was 15.7 ± 3.5 mSv (effective dose range: 9.1–19.6 mSv) in our study. The measured organ dose was

compared with that of the standard thoracic helical CT (collimation of 1.5 mm, a slice thickness of 5 mm, a pitch of 1.5, 0.5 second rotation time, 120 kVp, 200 mA) at our institution (17). The exposed radiation dose on HDCT was 30–40 mGy and the dose with performing standard thoracic helical CT was 15–20 mGy, which is similar to that reported elsewhere (15).

Evaluation of Enhancement Dynamics

The attenuation value of the nodule was measured on all the images at each time (from the unenhanced image to image acquired at 300 seconds) except for two sections (the upper most and lowest) and the maximum diameter of the SPN was obtained. An ROI covering approximately the full diameter of the nodule, but excluding calcified, cystic or necrotic areas was examined (Fig. 1). The edges of
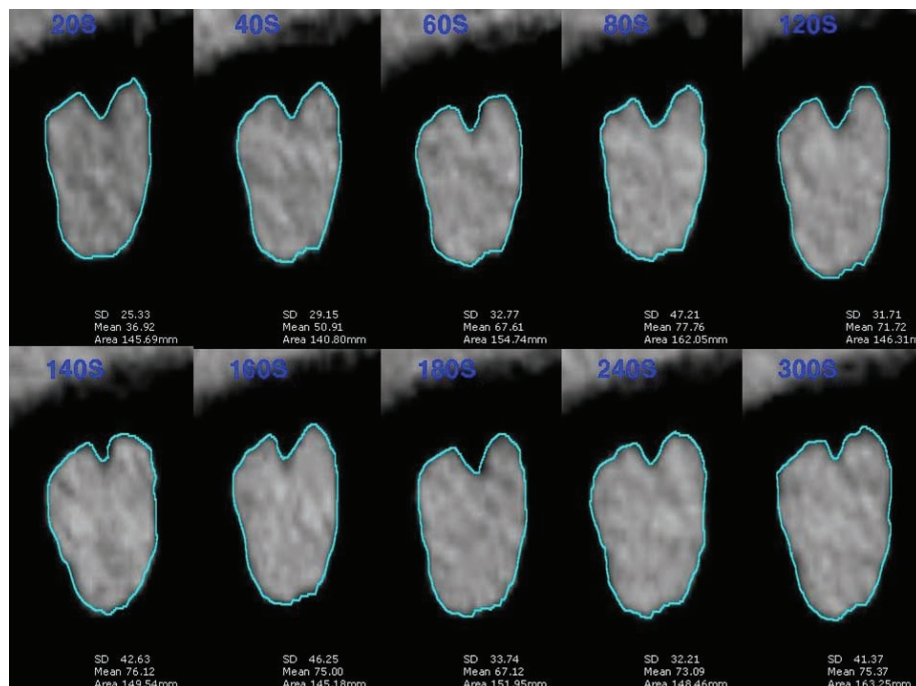
Fig. 1. Methods of enhancement pattern analysis using CAD system.
A. Before intravenously injecting contrast medium, series of images was obtained throughout entire nodule along z-axis, and additional ten sets (20s, 40s, 60s, 80s, 120s, 140s, 160s, 180s, 240s and 300s) of images were obtained at 20-second intervals over 5-minute period after injecting contrast medium. Region of interest covered approximately full diameter of nodule and single radiologist directly drew region of interest.
B. Solitary pulmonary nodule was region of interest drawn by expert technician with using CAD system.

the nodule were avoided in order to prevent partial volume averaging. All the measurements in Hounsfield units were obtained from the mediastinal window images to minimize partial volume averaging. All the measurements were obtained at the time of the CT examination without the radiologist having knowledge of the histologic diagnosis. One radiologist (prospective) with seven years experience of directly drawing ROIs and one technician (retrospective) with 20 years experience with chest CT and using a CAD system (Lung care, Sensation 16, Siemens, Germany) measured the attenuation values of the SPNs. For each image in which a nodule appeared, an ROI was identified by a well trained technician and using a semi-automated procedure in order to get the best possible segmentation. The technician initiated the ROI generation by selecting a point within the nodule. For all nodules, the ROIs were created, reviewed and edited by a well trained technician and once they were found to be satisfactory, the ROIs were approved by the thoracic radiologist (Fig. 1). The attenuation value of the nodule obtained from the ROI was obtained by averaging the measured values in all section. The enhancement of the SPN was evaluated according to the peak enhancement (PE), the net enhancement (NE) and the time attenuation curve (TAC) on the dynamic CT. The PE was defined as the maximum attenuation value of the nodule over the entire duration of the dynamic study. The NE was calculated by subtracting the

pre-enhancement attenuation from the PE attenuation. In this study, the TAC was classified into two types, that is, benign and malignant. The benign patterns included persistent enhancement < 15 HU and no wash-out or < 25 HU wash-out. The malignant patterns included early enhancement > 15 HU and early wash-out of 5–25 HU.

Data and Statistical Analysis

Statistical analyses were performed by using SPSS 9.0 software (SPSS Inc., Chicago, IL). The diagnostic characteristics such as sensitivity, specificity, accuracy, positive predictive value (PPV) and negative predictive value (NPV) were calculated retrospectively by considering the NE that signified a positive test (malignant with 15 HU or more of NE as a cutoff) for a dynamic CT. Additionally, the diagnostic characteristics were calculated by considering the TAC that signified a positive test (malignant with early enhancement > 15 HU and early wash-out of 5–31 HU) on a dynamic CT scan. Fisher's exact test and paired t-tests were used to analyze statistically significant differences between the malignant and benign nodules. Moreover, this study used Bland and Altman plots (26) to compare the numerical values of enhancement (PE and NE) between using CAD systems and those obtained by direct personal drawing. Having calculated the mean difference and the 95% limits of agreement, the investigators determined if the methods were sufficiently in
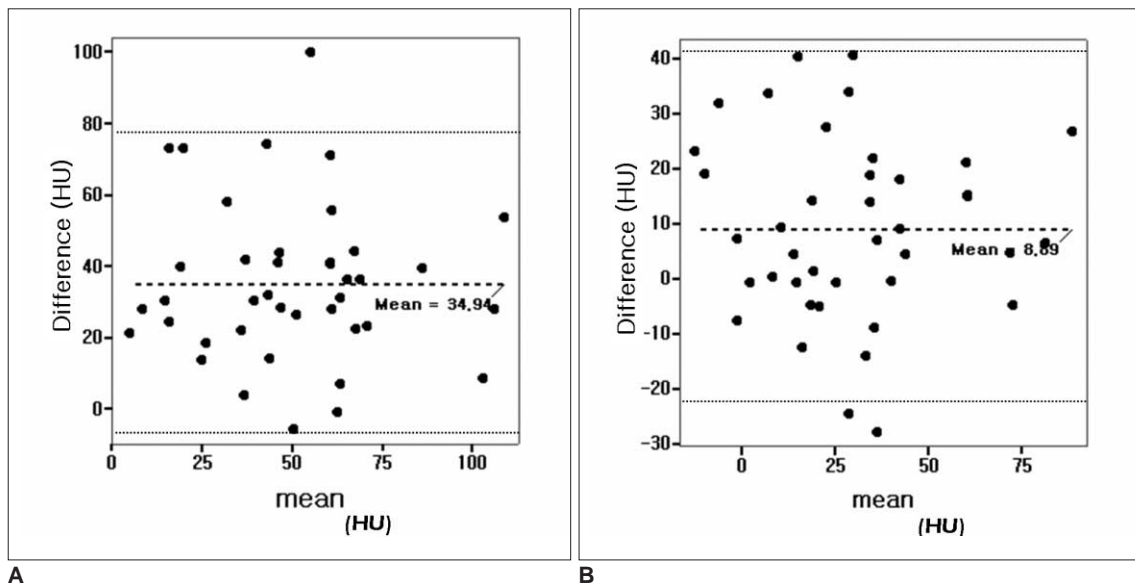

Fig. 2. Bland and Altman plot showing difference between using CAD system and direct personal drawing.
A. Difference in peak enhancement between using CAD system and direct personal drawing.
B. Difference in net enhancement between using CAD system and direct personal drawing. X-axis represented average values of using CAD system and direct personal drawing while y-axis represented difference in peak enhancement and net enhancement between using CAD system and direct personal drawing. Dashed lines represent mean value of two measurements and lines above and below it represent 95% limits of agreement. Peak enhancement was out of 95% limits of agreement only in one case, while net enhancement was out of 95% limits of agreement in two cases.

agreement for the new method to be used as an alternative.

RESULTS

There were 13 malignant SPNs and 27 benign SPNs. The malignant SPNs consisted of the following: adenocarcinoma (n = 8), squamous cell carcinoma (n = 2), bronchioloalveolar cell carcinoma (n = 1), mucoepidermoid carcinoma (n = 1) and carcinoid tumor (n = 1). The benign SPNs were tuberculosis (n = 9), focal bronchopneumonia (n = 7), hamartoma (n = 5), fungal infection (n = 2), intrapulmonary lymph node (n = 1), fibrotic nodule (n = 2) and sclerosing hemangioma (n = 1). Thirty SPNs included no calcification and 10 included puntated calcification.

Higher PE and NE were observed by direct personal drawing and by using the CAD system (Table 1). As seen from the numerical value of the enhancement of the PE and NE, direct personal drawing showed higher enhancement than did the CAD system. There were differences (mean: 34.9 HU; 95% CI: 28.0–41.8) between the PE using CAD systems (mean: 67.2 ± 27.1 HU) and the PE using the direct personal drawing (mean: 32.3 ± 28.1 HU). In addition, there were differences (mean: 6.9 HU, 95% CI: 1.1–12.7) between the NE using the CAD systems (mean: 25.9 ± 27.4 HU) and the NE using direct personal

drawing (mean: 32.8 ± 24.9 HU). On the other hand, as found from the enhancement patterns of PE and NE, the Bland and Altman plot showed that the mean difference was 95% of the individual differences ± 2 standard deriation (SD) (Fig. 2). With 15 HU or more of NE as a cutoff value for differentiating malignant and benign nodules, the sensitivity for the diagnosis of malignant SPNs using the CAD system was 92% (12/13), the specificity was 52% (14/27), the PPV was 48% (12/25), the NPV was 93% (14/15) and the accuracy was 65% (26/40), respectively. However, the sensitivity, specificity, PPV, NPV and the accuracy obtained by direct personal drawing of malignant SPNs was 100% (13/13), 37% (10/27), 43% (13/30), 100% (10/10), and 58% (23/40), respectively (Table 2).

On the other hand, of the 27 benign nodules, the CAD system and direct personal drawing of 25 nodules (92.6%) showed a similar TAC (Fig. 3). Of the 13 malignant nodules, the CAD system and direct personal drawing of 10 nodules (83.3%) showed a similar TAC (Fig. 4). The sensitivity, specificity, PPV, NPV and accuracy obtained by the TAC of the malignant SPNs and using CAD was 92% (12/13), 85% (23/27), 75% (12/16), 96% (23/24) and 88% (35/40), respectively. The sensitivity, specificity, PPV, NPV and accuracy obtained by the TAC of the malignant SPNs and using direct drawing was 92%

Table 1. Comparison of Peak Enhancement and Net Enhancement for Evaluating Solitary Pulmonary Nodules with Direct Personal Drawing and CAD System on Helical Dynamic CT

Characteristic	Mean ± SD (HU)	Median (HU)	95% Confidence Interval
PE			
Manual	67.2 ± 27.1	65.6	58.8–75.6
CAD	32.3 ± 28.1	32.7	23.6–41.0
Difference	34.9 ± 22.2	30.7	28.0–41.8
NE			
Manual	32.8 ± 24.9	28.7	25.1–40.5
CAD	25.9 ± 27.4	24.4	17.4–34.4
Difference	6.9 ± 18.7	7.1	1.1–12.7

Note.— Differences of PE and NE were calculated by subtracting PE and NE, with using CAD system, from manual PE and NE. CAD = computer-aided diagnosis, PE = peak enhancement, NE = net enhancement, SD = standard deviation.

Table 2. Comparison of Consistency of Various Parameters between CAD System and Direct Drawing of Regions of Interest on Helical Dynamic CT

Parameter	Accuracy (%)	Sensitivity (%)	Specificity (%)	PPV (%)	NPV (%)
NE (DR)	57.5	100	37.0	43.3	100
NE (CAD)	65.0	92.3	51.9	48.0	93.3
TAC (DR)	88.0	92.3	88.9	78.6	92.3
TAC (CAD)	88.0	92.3	85.2	75.0	96.0

Note.— * We used to Fisher's exact test. NE = net enhancement, TAC = time attenuation curve, DR = direct drawing, CAD = computer-aided diagnosis, PPV = positive predictive value, NPV = negative predictive value
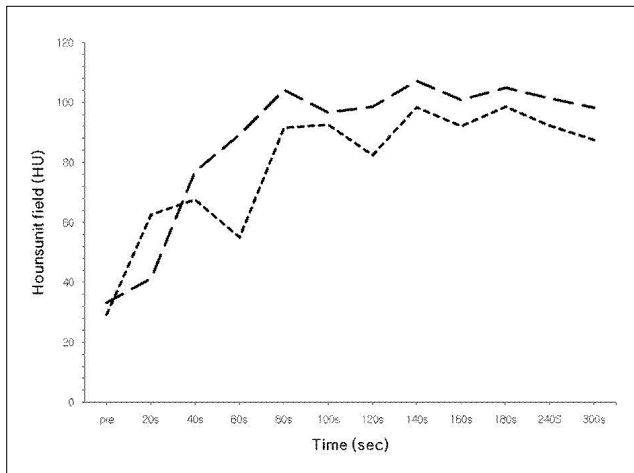
Fig. 3. CT scan of a benign solitary pulmonary nodule with enhancement (≥15 HU wash-in, ≥25 HU washout) in 43-year-old female diagnosed with sclerosing hemangioma by open lung biopsy. Time attenuation curve obtained through nodule for 5 minutes showed similar enhancement patterns of CAD system (short line) and direct personal drawing (long line).

Fig. 4. CT scan of adenocarcinoma with enhancement (≥15 HU wash-in, 5–25 HU washout) in 72-year-old man. Time attenuation curve obtained through nodule for 5 minutes showed similar enhancement patterns of CAD system (short line) and direct personal drawing (long line).
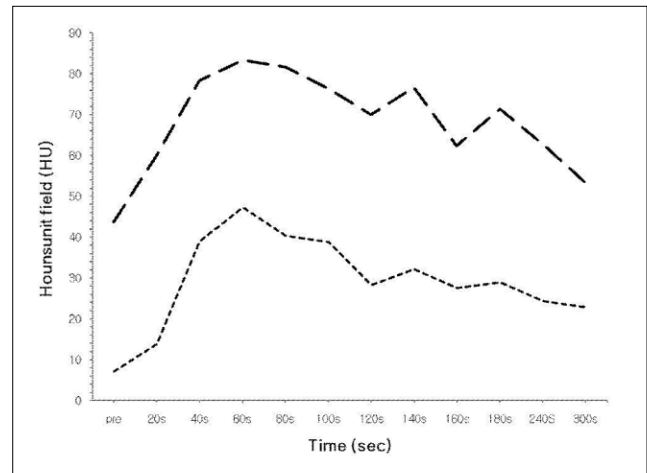
(12/13), 89% (24/27), 79% (14/16), 92% (24/26) and 88% (35/40), respectively.

DISCUSSION

In this study, the analysis of the TAC using the CAD system and the results of the direct personal drawing produced good results for making the diagnosis of malignant SPNs on HDCT, as compared with the using the PE and NE. The increase in attenuation of an SPN after contrast media injection, that is, the PE and NE, depends on the blood supply and the volume of the extravascular fluid in the SPN. However, the TACs of the SPNs represented differences in vascularity, the volume of extracellular fluid and the diffuse spread of contrast media. More contrast medium is delivered in malignant SPNs and the diffusion is faster compared with those of benign SPNs. For that reason, for better diagnostic accuracy of SPNs, the assessment of SPNs should be performed during the wash-out of contrast medium through the SPN in addition to the wash-in, the so called TAC. The TAC analyses using the CAD system showed similar specificity and accuracy to that of direct personal drawing. Therefore, the use of the CAD system for HDCT images to evaluate the TAC should help the thoracic radiologist differentiate between benign and malignant SPNs by reducing the time to calculate the SPN enhancement via negating the requirement to draw the ROIs for all the enhancing nodules on the CT images (1, 6–7, 10, 15).

Swenson et al. (14) reported that cutoff values of 15 HU produced a sensitivity of 98%, a specificity of 58% and an accuracy of 77% for malignant nodules. Since then, the cutoff value for diagnosing malignant nodules had been set at 15 HU. However, Jeong et al. (15) reported that when the diagnostic criteria for malignancy of both a wash-in phase of 25 HU or greater and a washout phase of 5–31 HU were applied, the sensitivity, specificity and accuracy for malignancy were 94%, 90% and 92%, respectively. Higher PE was obtained in the malignant SPNs for which multi-detector row CT (MDCT) was used, and thus, higher attenuation values could be used as cutoff values for this differentiation. For differentiating malignant and benign nodules in our study, the cutoff value of the enhancing SPNs was determined to be 15 HU because the PE with using CAD was lower than that of direct personal drawing in spite of performing MDCT. We thought that the cutoff value to evaluate malignant SPNs could change according to the type of CT scan that's used or the type of measurement that is used for the SPNs.

In the past decade, many studies have reported that CAD systems can help the radiologist detect SPNs on CT images (18–24). Das et al. (12) reported that the radiologists' performance in interpreting the multi-detector row CT scans can be improved using CAD systems. They compared the effect of two CAD systems, the Image Checker CT (R2 Technologies, Sunnyvale, CA) and the Nodule Enhanced Viewing (NEV) (Siemens Medical Solutions, Forchheim, Germany) for the detection of SPN. Regardless of the type of CAD system used, they showed that the CAD system might provide a more accurate diagnosis of SPNs. Lee et al. (21) showed that the sensitivities of the CAD system for detecting nodules < 5 mm in

diameter were higher than those of a radiologist. They suggested that the CAD system can help a radiologist detect nodules. Kim et al. (22) showed that a CAD system may help improve the detection of nodules with ground-glass opacity or localized ground-glass opacity. However, most studies have focused on the size of the SPN and not the SPN's enhancement. In this study, the TAC using the CAD system showed better results for diagnosing a malignant SPN than visually evaluating the PE and NE. It is well known that the hemodynamic differences are significant because malignant nodules tend to be more enhanced than benign nodules. There have been some studies designed to evaluate using the enhancement pattern of the HDCT images for diagnosing SPNs with employing a CAD system. For this approach, some studies used a number of parameters to evaluate the SPNs with employing a CAD system, e.g., the volumetric size, shape, enhancement etc (12, 18–20). Shah et al. (18) have recently used parameters such as the mean HU value, the median, mode and mean of the 32 highest HU values in the ROI etc. The major difficulty with this approach is that the analysis is limited to a single slice and the analysis was restricted to only the two-dimensional features. Therefore, in that study, the reviewing radiologist identified the most visually representative slice of the nodule and he drew the ROIs of the SPNs, while this experiment was performed helically through the entire nodule. This could result in a difference in diagnostic accuracy between the CAD system and the radiologist's direct drawing.

This study evaluated the enhancement patterns of HDCT images with using a CAD system. In general, direct personal drawing tended to show higher enhancement than did the CAD system because the radiologist tried to perform direct drawing within the SPN as much as possible, but the CAD system included lung parenchyma for detecting a SPN when calculating the enhancement's properties. As seen from the numerical value of the enhancement of the PE and NE, it seems that there is a difference between CAD system and direct personal drawing. On the other hand, the Bland-Altman plot showed that the analyses of the PE and the NE using the CAD system produced similar results to those obtained with direct personal drawing. Moreover, there was uniform variability throughout the range of measurements. Some studies showed that the sensitivity and specificity of a CAD system were lower than those of direct personal drawing because those studies used the morphologic character rather than the enhancement pattern of the SPN (18–20, 23, 24). But our study used the enhancement pattern of HDCT images with using the CAD system to evaluate the SPNs. Therefore, unlike the previous studies,

this study showed that the accuracy and specificity of a CAD system was similar with that of direct personal drawing.

Although the CAD system is a useful tool for improving the radiologist's performance, the CAD system has a major drawback in that the SPN cannot be differentiated from small peripheral vessels, most commonly branch points, scarring or other parenchymal heterogeneities. Therefore, if the SPN is a juxtavascular nodule, then the CAD system might calculate the enhancement pattern of both the SPN and it vascular component. In the case of a small sized SPN, it is difficult to calculate the enhancement pattern of the SPN with using a CAD system. This might produce a false enhancement pattern of the SPN. According, we excluded those cases in this study.

There were some limitations in the study. First, there was an insufficient the number of cases (n = 40). Therefore, before any type of clinical use could be considered, this proposed method will need to be validated on a larger dataset, i.e., more cases will be needed to test for generality. Accordingly, examination of more nodules of various sizes and shapes by CT will be needed for additional training and testing. Second, although the variability in the ROIs of interest is substantial between radiologists, this was not evaluated in our study. The inadequate placement of the ROIs of interest on nodules might result in erroneous attenuation values, which can cause false wash-in and washout enhancement calculations. Third, 5-minutes was chosen as the length for the delay as a rule of thumb, which we believe is sufficient for the washout of the contrast material from a pulmonary nodule. Jeong et al. (1) reported that the mean time to PE in most malignant nodules was 3.2 minutes. In addition Yi et al. (10) reported that most SPNs reached the peak level of enhancement within 3 minutes. They reported that with images acquired during 5 minutes or more, the washout dynamics of the pulmonary nodule enhancement could be obtained. Therefore, 5 minutes was chosen as the length for the delay because the PE and NE were calculated and the pattern of the TAC differentiated between the malignant nodules and the benign nodules. In addition, there was no attempt to standardize the injection rate and the volume of contrast material according to the cardiac output of each patient nor was there any attempt to standardize the volume of contrast material according to the patients' weight. Moreover, the calculated dose at all sites of the nodule is not same due to a direct influence of the radiation dose, such as the X-ray beam energy, the tube current, rotation of exposure time, the section thickness, the object's thickness of attenuation, pitch, the sites of nodule etc. Therefore, for the larger patient, the exit

radiation would be much less intense due to its attenuation through more tissue (27). The calculated dose at all sites of the nodules in this study was 30–40 mGy and this result was similar to the calculated dose of other reports (1, 10).

Despite these limitations, the results obtained from the enhancement pattern of the SPNs using the CAD system were similar to those obtained by the direct personal drawing of SPNs. Consequently, the CAD system was a useful tool for diagnosing malignant solitary pulmonary nodules. Also, in view of the good diagnostic results for a malignant SPN, a TAC may be more useful than the PE or NE.

References

1. Jeong YJ, Yi CA, Lee KS. Solitary pulmonary nodules: detection, characterization, and guidance for further diagnostic workup and treatment. *AJR Am J Roentgenol* 2007;188:57-68
2. Leef JL 3rd, Klein JS. The solitary pulmonary nodule. *Radiol Clin North Am* 2002;40:123-143
3. Shaham D, Guralnik L. The solitary pulmonary nodule: radiologic considerations. *Semin Ultrasound CT MR* 2000;21:97-115
4. Tan BB, Flaherty KR, Kazerooni EA, Iannettoni MD. The solitary pulmonary nodule. *Chest* 2003;123:S89-S96
5. Tang AW, Moss HA, Robertson RJ. The solitary pulmonary nodule. *Eur J Radiol* 2003;45:69-77
6. Wang MP, Tan YQ, Zhang GZ, Zhang JG, Wu H, Yang JY. Differential diagnosis of benign and malignant solitary pulmonary nodule with computer-aided detection. *Zhongguo Yi Xue Ke Xue Yuan Xue Bao* 2006;28:64-67
7. Erasmus JJ, Connolly JE, McAdams HP, Roggli VL. Solitary pulmonary nodules: Part I. Morphologic evaluation for differentiation of benign and malignant lesions. *Radiographics* 2000;20:43-58
8. Marten K, Grabbe E. The challenge of the solitary pulmonary nodule: diagnostic assessment with multislice spiral CT. *Clin Imaging* 2003;27:156-161
9. Yankelevitz DF, Henschke CI. Small solitary pulmonary nodules. *Radiol Clin North Am* 2000;38:471-478
10. Yi CA, Lee KS, Kim BT, Choi JY, Kwon OJ, Kim H, et al. Tissue characterization of solitary pulmonary nodule: comparative study between helical dynamic CT and integrated PET/CT. *J Nucl Med* 2006;47:443-450
11. Trotman-Dickenson B, Baumert B. Multidetector-row CT of the solitary pulmonary nodule. *Semin Roentgenol* 2003;38:158-167
12. Das M, Mühlenbruch G, Mahnken AH, Flohr TG, Gündel L, Stanzel S, et al. Solitary pulmonary nodule: effect of two computer-aided detection systems on radiologist performance. *Radiology* 2006;241:564-571
13. Muhm JR, McCullough AE. The enhancing rim: a new sign of a benign pulmonary nodule. *Mayo Clin Proc* 2003;78:1092-1096
14. Swensen SJ, Viggiano RW, Midthun DE, Müller NL, Sherrick A, Yamashita K, et al. Lung nodule enhancement at CT: multicenter study. *Radiology* 2000;214:73-80
15. Jeong YJ, Lee KS, Jeong SY, Chung MJ, Shim SS, Kim H, et al. Solitary pulmonary nodule: characterization with combined wash-in and washout features at dynamic multi-detector row CT. *Radiology* 2005;237:675-683
16. Schaefer JF, Vollmar J, Schick F, Vonthein R, Seemann MD, Aebert H, et al. Solitary pulmonary nodules: dynamic contrast-enhanced MR imaging—perfusion differences in malignant and benign lesions. *Radiology* 2004;232:544-553
17. Yi CA, Lee KS, Kim EA, Han J, Kim H, Kwon OJ, et al. Solitary pulmonary nodules: dynamic enhanced multi-detector row CT study and comparison with vascular endothelial growth factor and microvessel density. *Radiology* 2004;233:191-199
18. Shah SK, McNitt-Gray MF, Rogers SR, Goldin JG, Suh RD, Sayre JW, et al. Computer aided characterization of the solitary pulmonary nodule using volumetric and contrast enhancement features. *Acad Radiol* 2005;12:1310-1319
19. Shah SK, McNitt-Gray MF, Rogers SR, Goldin JG, Suh RD, Sayre JW, et al. Computer-aided diagnosis of the solitary pulmonary nodule. *Acad Radiol* 2005;12:570-575
20. Mori K, Niki N, Kondo T, Kamiyama Y, Kodama T, Kawada Y, et al. Development of a novel computer-aided diagnosis system for automatic discrimination of malignant from benign solitary pulmonary nodules on thin-section dynamic computed tomography. *J Comput Assist Tomogr* 2005;29:215-222
21. Lee JW, Goo JM, Lee HJ, Kim JH, Kim S, Kim YT. The potential contribution of a computer-aided detection system for lung nodule detection in multidetector row computed tomography. *Invest Radiol* 2004;39:649-655
22. Kim KG, Goo JM, Kim JH, Lee HJ, Min BG, Bae KT, et al. Computer-aided diagnosis of localized ground-glass opacity in the lung at CT: initial experience. *Radiology* 2005;237:657-661
23. Goo JM, Lee JW, Lee HJ, Kim S, Kim JH, Im JG. Automated lung nodule detection at low-dose CT: preliminary experience. *Korean J Radiol* 2003;4:211-216
24. Rubin GD, Lyo JK, Paik DS, Sherbondy AJ, Chow LC, Leung AN, et al. Pulmonary nodules on multi-detector row CT scans: performance comparison of radiologists and computer-aided detection. *Radiology* 2005;234:274-283
25. Verdun FR, Gutierrez D, Schnyder P, Aroua A, Bochud F, Gudinchet F. CT dose optimization when changing to CT multi-detector row technology. *Curr Probl Diagn Radiol* 2007;36:176-184
26. Bland JM, Altman DG. Statistics methods of assessing agreement between two methods of clinical measurement. *Lancet* 1986;1:307-310
27. McNitt-Gray MF. AAPM/RSNA physics tutorial for residents: topics in CT. Radiation dose in CT. *Radiographics* 2002;22:1541-1553